Journal of Applied Polymer Science

Preparation and hemocompatibility of electrospun O-carboxymethyl chitosan/PVA nanofibers

Qinghuan Zeng,[1] Jinmin Qin,[1] Xueqiong Yin,[1] Haifang Liu,[2] Li Zhu,[1] Wenyuan Dong,[1] Song Zhang[1]

[1]Hainan Provincial Fine Chemical Engineering Research Center, Hainan University, Haikou Hainan 570228, People's Republic of China

[2]Affiliated Haikou Hospital, Xiangya School of Medicine central south University, Haikou Municipal People's Hospital, Haikou Hainan 570208, People's Republic of China

Correspondence to: X. Yin (E-mail: yxq88@hotmail.com)

ABSTRACT: Chitosan was deacetylated and carboxymethylated to prepare O-carboxymethyl chitosan (CMC) for further electrospinning. CMC was characterized using FTIR, NMR, and chemical titration, indicating a degree of carboxymethylation of 51.4%. CMC was electrospun together with poly(vinyl alcohol) (PVA) to prepare membranes composed of nanofibers. The electrospinning conditions were optimized. The CMC/PVA membrane obtained at the conditions of 15.2 g/mL CMC 50 mL, 8 g/mL PVA 5 mL, 25 kV, and a distance of 23 cm, had nanofibers without beads, with diameters of 70–200 nm. The mats were crosslinked by glutaraldehyde before platelet adhesion measurement. The nanofibrous structure remained after crosslinking while the wettability decreased. CMC/PVA mats with higher CMC amount and fewer beads, had fewer adherent platelets and less platelets aggregation showing better hemocompatibility. © 2016 Wiley Periodicals, Inc. J. Appl. Polym. Sci. **2016**, *133*, 43565.

KEYWORDS: biocompatibility; biopolymers & renewable polymers; electrospinning; nanostructured polymers; polysaccharides

Received 11 October 2015; accepted 18 February 2016
DOI: 10.1002/app.43565

INTRODUCTION

Nonwoven fabric composed of nanofibers is getting increasing attention in the field of biomaterials owing to its structural similarity to the native extracellular matrix.[1,2] Diameters of nanofibers are defined as less than 100 nm, sometime extended to 1000 nm. The nanostructure and resulting unique properties make the nonwoven fabric popular in biomaterials, such as tissue engineering scaffolds, drug delivery, wound dressings, antibacterial coatings, biosensors, artificial organs, implant materials, medical textiles etc.[3–5]

Electrospinning is an attractive method for preparing nonwoven fabrics composed of nanofibers. The fibers from electrospinning usually have diameters in the range of 40 nm to 2 μm.[6,7] During the process of electrospinning, a high voltage is applied to the solution droplet and the droplet undergoes an electrostatic repulsion force. When the electrical force at the interface of droplet overcomes the surface tension, a stream of liquid erupts from the droplet surface. Very fine fibers are formed from the erupted liquid after the solvent evaporating during flying. Electrospinning membrane usually has high surface area, high porosity, and ultrafine fibers. The special morphology makes electrospun membrane a potential material in the fields of filtration, enzyme immobilization, sensors, electroconductor, and especially biomaterials.[8–10] The morphology of electrospinning membrane is affected by many factors, such as chemical constituents, material structure (molecular weight, solution viscosity and conductivity), solvent, voltage, distance, etc.[6,7,9,11] An expected nanostructure may be achieved through adjusting the above factors.

Chitin (poly-β-1,4-D-N-acetylglucosamine) is the second most abundant natural polysaccharide on earth whose total annual production is about 1 to 100 billion ton and 1.5 million tons available for commercial application.[12] Chitosan is the N-deacetylated derivative of chitin, having good physicochemical and biochemical properties, such as good biocompatibility, biodegradability, antibacterial and antifungal activities, moisture absorption etc.[13] Carboxymethyl chitosan is the most popular derivative of chitosan, also widely investigated in the field of biomaterials. Electrospinning of chitosan and carboxymethyl chitosan has been investigated in recent years.[14,15] Owing to the strong molecular interaction between the high charge density and high viscosity of chitosan and CMC solutions, it is very difficult to electrospin chitosan or CMC solely.[16,17] Other polymers having flexible polymer chain can be electrospun easily, such as poly(vinyl alcohol) (PVA), polyethylene oxide (PEO). Those polymers have been used to support the electrospinning of chitosan to prepare nanofibers from chitosan.[18–21]

Hemocompatibility (blood compatibility) is a key property determining the potential of using blood-contacting biomaterial. A good blood compatible material should not lead to the activation of the blood coagulation cascade. The process of blood coagulation is induced by a foreign material characterized by plasma proteins first non-specifically adsorbing onto the foreign material surface, causing platelet activation, adhesion and aggregation, and then resulting in blood coagulation.[22] Therefore, protein adsorption and platelet adhesion are two critical processes.[23] The surface structure characteristics of foreign material (chemical component, morphology, surface charge, surface wettability, etc.) play key roles for the whole coagulation process.[24] Negatively charged material surfaces have good hemocompatibility owing to electrostatic repulsion between the platelet and the material surface.

The hemocompatibility of chitosan is controversial because chitosan can elicit many different bioresponses, such as electrostatic attraction between its net positive charge and negatively charged fibrinogen resulting in protein adsorption.[25] Therefore, in this work, chitosan was modified to prepare hemocompatible derivatives. Chitosan derivatives with negative —SO_3H or —COOH group have been shown to express good hemocompatibility.[26,27] The electrostatic repulsion between the negatively charged groups and fibrinogen retards fibrinogen adsorption which is responsible for the formation of a fibrin network, platelet adsorption, blood cell trapping, and coagulation. The origin, degree of N-deacetylation (DD), molecular weight (MW), distribution and substitution degree of the derivative all have affects on the bioactivity of chitosan derivatives.[26] Measurement of the hemocompatibility of chitosan and CMC is usually carried out with solution, while that of their nanofibers has not been reported until now.[28]

In this work, chitosan was completely deacetylated to reduce the influence of DD on chitosan modification and the hemocompatibility of the derivative. Deacetylated chitosan was carboxymethylated with chloroacetic acid at lower temperature to prepare O-carboxymethyl chitosan (CMC). The obtained CMC was electrospun with PVA to prepare nanofibrous membranes (CMC/PVA), followed by crosslinking with glutaraldehyde. The structure of the electrospun membrane was characterized with SEM, FTIR, and water contact angle measurement. The hemocompatibility of the membrane was measured through platelet adhesion. This is the first report focused on hemocompatibility of nanofiber CMC. The CMC/PVA membrane has the potential to be applied in blood-contact biomaterials, such as wound dressings and drug delivery.

EXPERIMENTAL

Materials

Chitosan was purchased from Zhejiang Golden Shell Biological Chemical Co., Ltd. (M_w 5 × 10^5 g/mol, DD 78%). Dimethyl sulfoxide (DMSO), hexadecyl trimethyl ammonium bromide (HTAB), sodium hydroxide (NaOH), monochloroacetic acid, NaH_2PO_4, $NaH(PO_4)_2$, and 25% glutaraldehyde solution were purchased from Sinopharm Group Company Limited (China) and used as received. PVA (99% hydrolyzed, Mw 120,000 g/mol) was purchased from Sigma-Aldrich.

Preparation of Completely Deacetylated Chitosan (DCT)

Chitosan was completely deacetylated as described previously.[29] 10 g chitosan was added into a 500 mL three-neck flask containing a pre-dissolved mixture of 200 mL DMSO, 20 g NaOH, and 0.4 g HTAB. The reaction was allowed for 3 h at 130 °C under the protection of nitrogen. Then the reaction mixture was cooled to room temperature, filtered, washed with distilled water until neutral, and then lyophilized. White DCT was obtained and used for carboxymethylation.

Preparation of O-Carboxymethyl Chitosan (CMC)

CMC was produced as described in reference.[30] 20 mL 40% NaOH solution was dropped into a 2 g DCT in a 100 mL beaker to alkalize DCT. The chitosan NaOH mixture was frozen at −18 °C overnight, and then thawed. 20 mL isopropanol was added to the thawed chitosan mixture and then 9.6 g monochloroacetic acid in 20 mL isopropanol was dropped into chitosan under stirring at 30 °C. The reaction was allowed for 4 h, followed by neutralization with diluted hydrochloric acid. The mixture was precipitated in ethanol. White powder CMC was obtained after filtration, washed alternatively with 80% methanol and ethanol, and finally vacuum dried at 50 °C for 6 h. The degree of carboxymethylation was determined through titration.[31]

Electrospinning of CMC/PVA

CMC solutions with different concentration were prepared by dissolving CMC in water with stirring. PVA solution (8 wt %) was prepared in distilled water at 80 °C with constant stirring for at least 2 h. The polymer solutions were mixed in different proportions (the mass ratio of CMC to PVA varied from 10: 1 to 18.75 : 1) with 0.1 g NaCl by intense stirring, resulting in a homogeneous CMC/PVA blend. The electrospinning experiment was carried out on an electrostatic spinning instrument (DT-200, Dalian Dingtong technology development Co., Ltd.). In a typical procedure, the polymer blend solution was put into a 25 mL syringe and delivered to the tip of the syringe needles by the syringe pump at a constant feed rate (0.7 mL/h). A positive voltage of 20 kV was applied to the polymer solution via the stainless steel syringe needle. The distance between the tip of the needle and the collector was maintained at 20 cm. The electrospun polymer fibers were collected on a collector covered with aluminum foil. Electrospun mats of CMC/PVA were cut into a square shape with dimensions of 10 cm × 10 cm for crosslinking. The electrospun membranes were further crosslinked using a vapor of glutaraldehyde from a 25% glutaraldehyde aqueous solution at room temperature for 2 days. After crosslinking, the membranes were treated with a 0.1 M glycine aqueous solution to block unreacted aldehyde groups.

Characterization of CMC/PVA Membrane

The surface morphology of the CMC/PVA mats was observed with a S-3000 N scanning electron microscope after gold coating, at a voltage of 10 kV. 30 fibers in the SEM images were randomly selected to measure the diameter with the software e-Ruler and the average diameter was calculated accordingly. Fourier transform infrared spectroscopy (FTIR) spectra were obtained on a TENSOR 27 spectrometer in the range of 500–4000 cm^{-1}. The nuclear magnetic resonance spectrum (NMR)

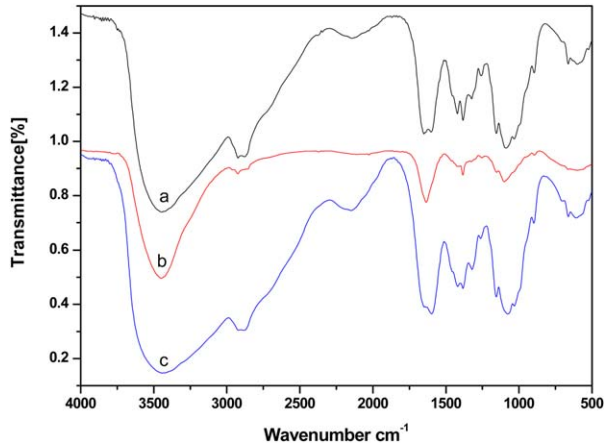

Figure 1. FTIR spectra of chitosan (a), deacetylated chitosan (b), and carboxymethyl chitosan (c). [Color figure can be viewed in the online issue, which is available at wileyonlinelibrary.com.]

was recorded on a Bruker AV 400 nuclear magnetic resonance spectrometer at 27 °C, using TMS as the internal standard. The water contact angles of the membranes were measured using a SL200K contact angle measurement instrument at 20 °C. A drop of deionized water was dropped onto the sample membranes. The contact angles were calculated using an image processing software CAST^{TM}2.0. The measurement was reproduced 10 times and the average value was used.

Platelet Adhesion Experiments

For the platelet adhesion experiments,[32] platelet-rich plasma (PRP) obtained from centrifuged human whole blood containing sodium citrate was used. 250 μL PRP was poured onto the CTS/PVA mats (0.5cm × 0.5cm) and allowed to maintain at 37 °C for 2 h. Then the samples were carefully washed with saline to remove the nonadhered blood cells. The adhered blood cells were fixed by immersing the mats into 20 mL 2.5 wt % solution of glutaraldehyde in PBS for 1 h at room temperature to fix the platelet. The film was washed with PBS and then subsequently dehydrated by immersing in a series of ethanol–water solutions [50, 60, 70, 80, 90, 95 and 100% (v/v)] for 30 min each and allowed to evaporate at room temperature. The sample was dried for further operation. The surface of the film was observed with a S-3000N scanning electron microscope after gold coating.

RESULTS AND DISCUSSION

Preparation and Characterization of O-Carboxymethyl Chitosan

Chitosan is deacetylated chitin with a degree of deacetylation (DD) more than 60%. The presence and random distribution of the acetyl group on the backbone of chitosan make the structure of chitosan complicated. Completely removing acetyl group can improve the biological activity of chitosan and eliminate the uncertain effect of the structure on the properties. Therefore, chitosan was first completely deacetylated with the assistance of surfactants[29] and then carboxymethylated to prepare CMC. The degree of carboxymethylation was 51.4% according to what was obtained from acid-base titration. The FTIR spectra of chitosan, deacetylated chitosan, and CMC are shown in Figure 1.

For chitosan (a), the peak at 1653 cm^{-1} was the characteristic absorbance of the amide-I band, and 1578 cm^{-1} was the bending vibration band of —NH_2. After deacetylation (b), the absorbance of the amide-I band around 1653 cm^{-1} disappeared, which indicated that chitosan had been deacetylated. The peak at 1070 cm^{-1} was due to the —C—O asymmetric stretching vibration. Compared with the spectrum of deacetylated chitosan (b), CMC (c) had an obvious peak around 1650 cm^{-1}, which was the overlapped peak from the asymmetric stretching of —C═O (—COONa) and the bending vibration band of —NH_2.[33] The new absorption peaks at 1468 cm^{-1} was assigned to the symmetry stretch vibration of COO^-.[29] The FTIR spectra indicated that chitosan was deacetylated and then carboxymethylated successfully.

Figure 2 shows the NMR spectra of deacetylated chitosan (a) and CMC (b) at room temperature. There was no signal around 175 ppm corresponding to the carbonyl carbon and that of methyl around 20 ppm in the spectrum of deacetylated chitosan, which indicated that chitosan had been completely deacetylated.[33] The characteristic signals of C-1, C-4, C-5, C-3, C-6, and C-2 appeared at 95.9, 74.8, 73.1, 68.4, 58.4, and 54.2 ppm.[34] Only one new peak at 167.0 ppm due to the C═O of carboxymethyl group and one at 45.6 ppm due to the methylene groups (—CH_2) of CH_2COO^- appeared in CMC spectrum, indicating that carboxymethylation only occurred at OH-6. These features demonstrated that chitosan had been completely deacetylated allowing tailored O-carboxymethylated chitosan to be obtained.

Electrospinning and Characterization of CMC and PVA

CMC was first dissolved in water to prepare CMC solutions of different concentrations. Owing to the high viscosity and electrostatic repulsion of CMC, it was hard to reach the necessary polymer entanglement for electrospinning while electrospinning CMC solely. Therefore, PVA having a flexible polymer chain and the facility to crosslink to CMC was used to enhance the electrospinning of CMC.[35] The samples were electrospun at 20

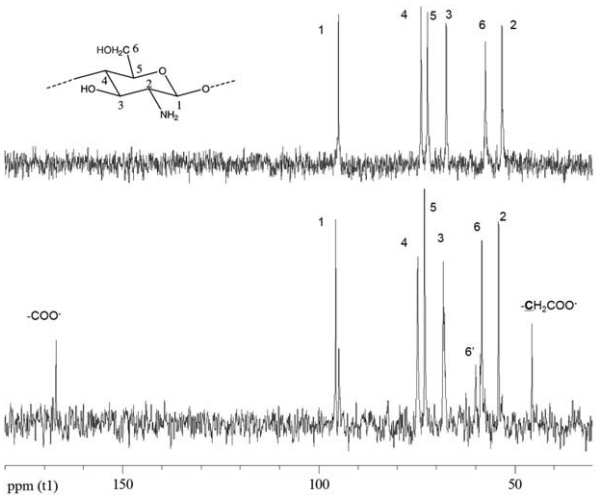

Figure 2. NMR spectra of deacetylated chitosan (a) and CMC (b).

Table I. Electrospinning Conditions of CMC/PVA

Samples	CMC[a] con (wt %)	PVA[b] (mL)	CMC:PVA (g:g)	Polymer con (wt %)[c]	Distance (cm)	Voltage (kV)
PVA	0	5	0:1	8.0	20	20
CMC1	7.3	5	10:1	8.9	20	20
CMC2	8.2	5	11.25:1	9.8	20	20
CMC3	9.1	5	12.5:1	10.7	20	20
CMC4	10.0	5	13.75:1	11.6	20	20
CMC5	11.0	5	15:1	13.5	20	20
CMC6	12.7	5	17.5:1	14.4	20	25
CMC7	13.6	5	18.75:1	14.7	20	25
CMC8	13.0	10	10:1	14.7	22	25
CMC9	15.2	10	11.25:1	16.3	23	25

[a] Volume of all the CMC samples was 50 mL.
[b] 8 wt % PVA was used.
[c] The concentration includes both CMC and PVA.

kV in the presence of 0.1 g NaCl. The electrospinning conditions are shown in Table I. The SEM images of CMC/PVA are shown in Figures 3 and 4.

PVA aqueous solution with a concentration of 8 wt % was electrospun alone. As shown in Figure 3, the nonwoven PVA mat contains randomly arranged and even distributed nanofibers with diameters of ~120 nm. When different amounts CMC were added to PVA, the morphology of the nonwoven mats varied with increasing CMC. When the concentration of CMC was 7.3 wt % (CMC1), there were few fibers—mostly beads in the mats. With an increase in the CMC amount, the fiber content increased and the fiber diameter decreased.[36] When the CMC concentration reached 9.1 wt % (CMC3), there were only a few beads in the mat and the diameter of fibers decreased to ~70 nm. However, further increasing the CMC amount resulted in thinner fibers and more beads (CMC4 and CMC5). When CMC concentration was low, there were not enough CMC molecules to entangle PVA, which resulted in less electrospinning efficiency. Furthermore, high CMC concentration can cause strong electrostatic repulsions and extended polymer chains, resulting in inefficient chain entanglement and low electrospinning efficiency. Therefore, when using higher CMC concentrations, a higher voltage and more PVA are required.

As shown in Table I (CMC6-CMC9), the voltage of CMC electrospinning was increased to 25 kV. The SEM images of CMC6-CMC9 are shown in Figure 4. The electrospinning efficiency of CMC/PVA increased with an increase in the CMC concentration. A CMC/PVA mat with 12.7 wt % CMC had bead

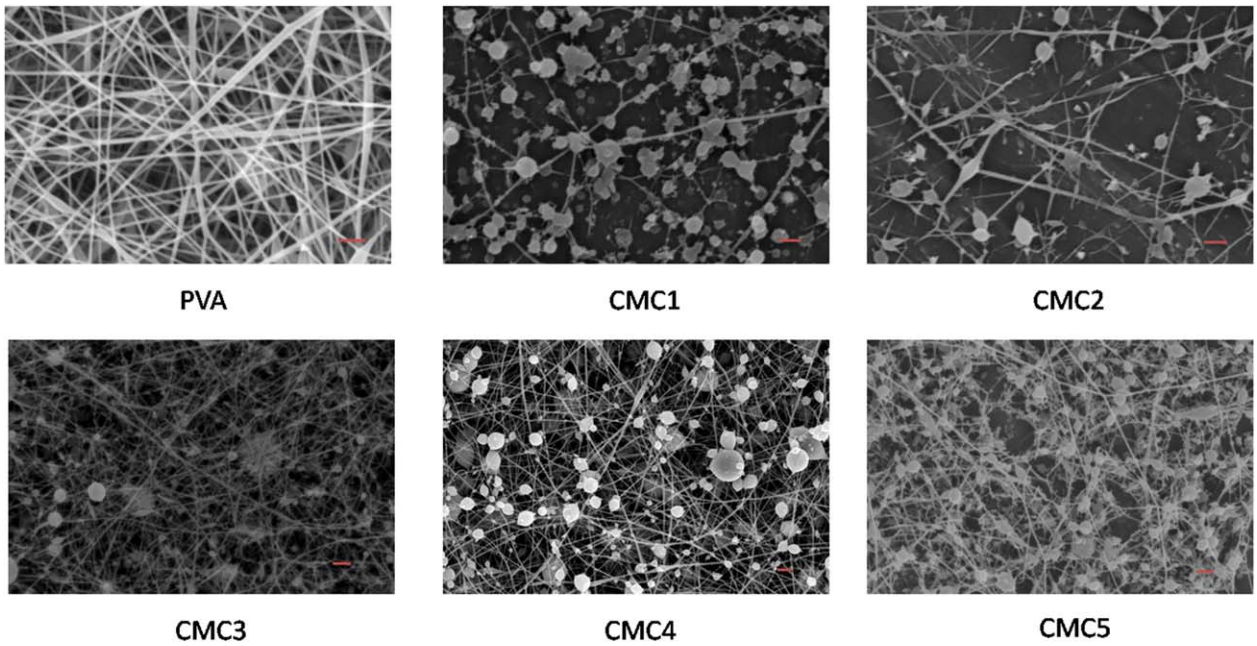

Figure 3. SEM images of PVA and CMC/PVA with different CMC concentration prepared at a voltage of 20 kV (the length of the scale bar is 1 μm). [Color figure can be viewed in the online issue, which is available at wileyonlinelibrary.com.]

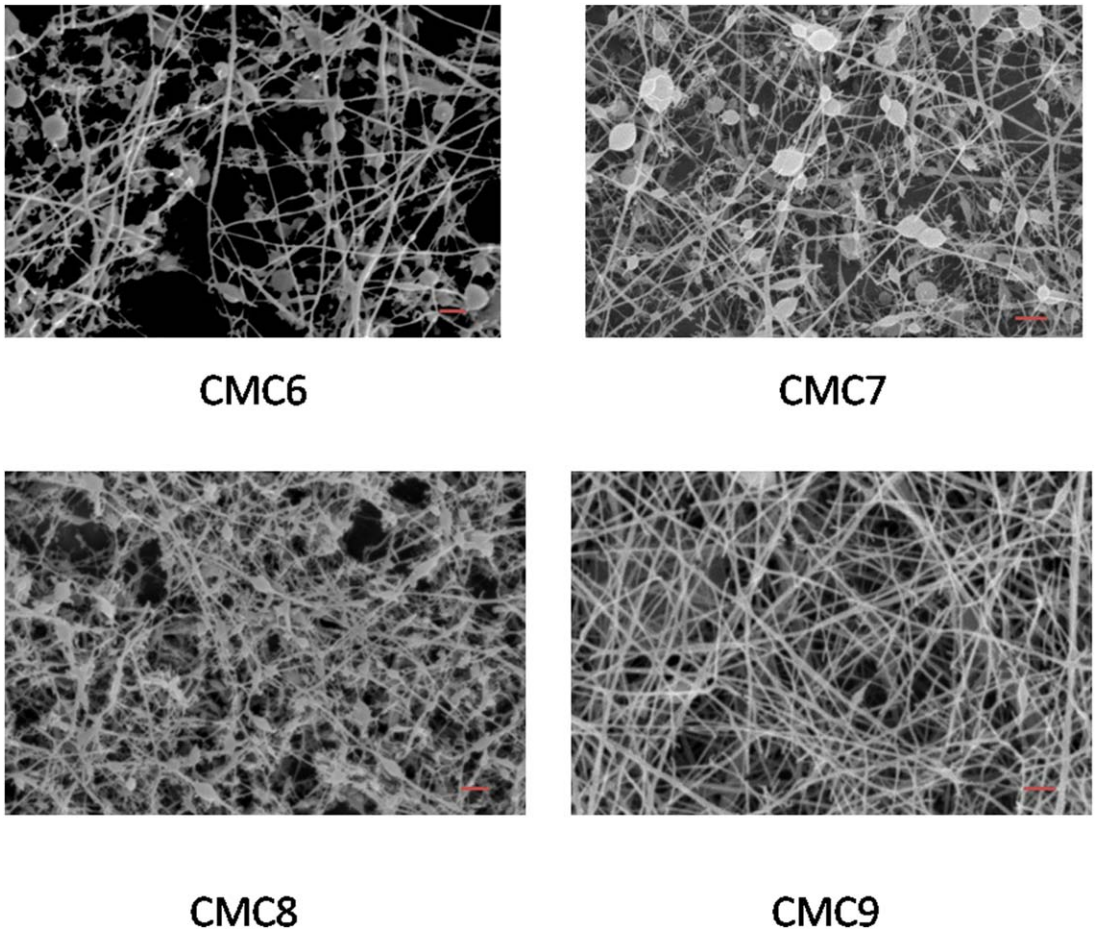

Figure 4. SEM images of CMC/PVA mats prepared at a voltage of 25 kV (the length of the scale bar is 1 μm). [Color figure can be viewed in the online issue, which is available at wileyonlinelibrary.com.]

morphology, while that with 13.6 wt % CMC in the mats showed a reduced bead morphology. Increasing PVA concentration can decrease the surface tension of PVA/CMC solution.[35] Therefore, the amount of PVA was increased to 10 mL for CMC8 and CMC9. CMC8 had a fibrous structure with very few beads. Increasing the CMC concentration to 15.2 wt %, CMC9 prepared at 25 kV at a distance of 23 cm showed pure nanofibers with a diameter of 100-200 nm. The results expressed for CMC/PVA mats, proper PVA amount and polymer concentration were necessary to guarantee CMC electrospinning.

Crosslinking and Platelet Adhesion of CMC/PVA Mats

Owing to the solubility of CMC in water, CMC/PVA mats were crosslinked with glutaraldehyde vapors to stabilize CMC for further hemocompatability. While crosslinking of CMC with glutaraldehyde, there are many possibilities. Firstly, one aldehyde group of glutaraldehyde undergoes a Schiff reaction with the $-NH_2$ group of CMC. Then, the second aldehyde group can undergo a second Schiff reaction with the $-NH_2$ group from the same CMC chain or another chain. Moreover, the second aldehyde group can also condense with another glutaraldehyde to form $-C=C-$.[37] $-C=C-$ is conjugated with C=N, which make the crosslinked polymer more stable. The existence of aliphatic chains, $-C=C-$, the reduction of the hydrogen bonding $-NH_2$ groups, and the flexibility of chitosan chain increase the hydrophobicity of the membrane.

Figure 5 is the FTIR spectra of PVA (a), CMC (b), CMC/PVA (CMC9, c), and crosslinked CMC/PVA (CMC9, d). The blend

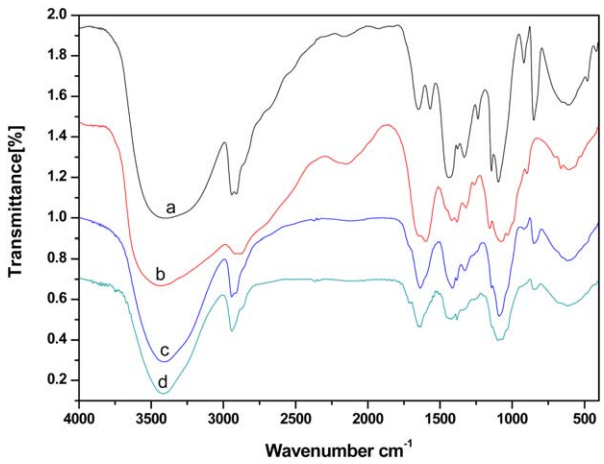

Figure 5. FTIR spectra of PVA (a), CMC (b), CMC/PVA (CMC9, c), and crosslinked CMC/PVA (CMC9, d). [Color figure can be viewed in the online issue, which is available at wileyonlinelibrary.com.]

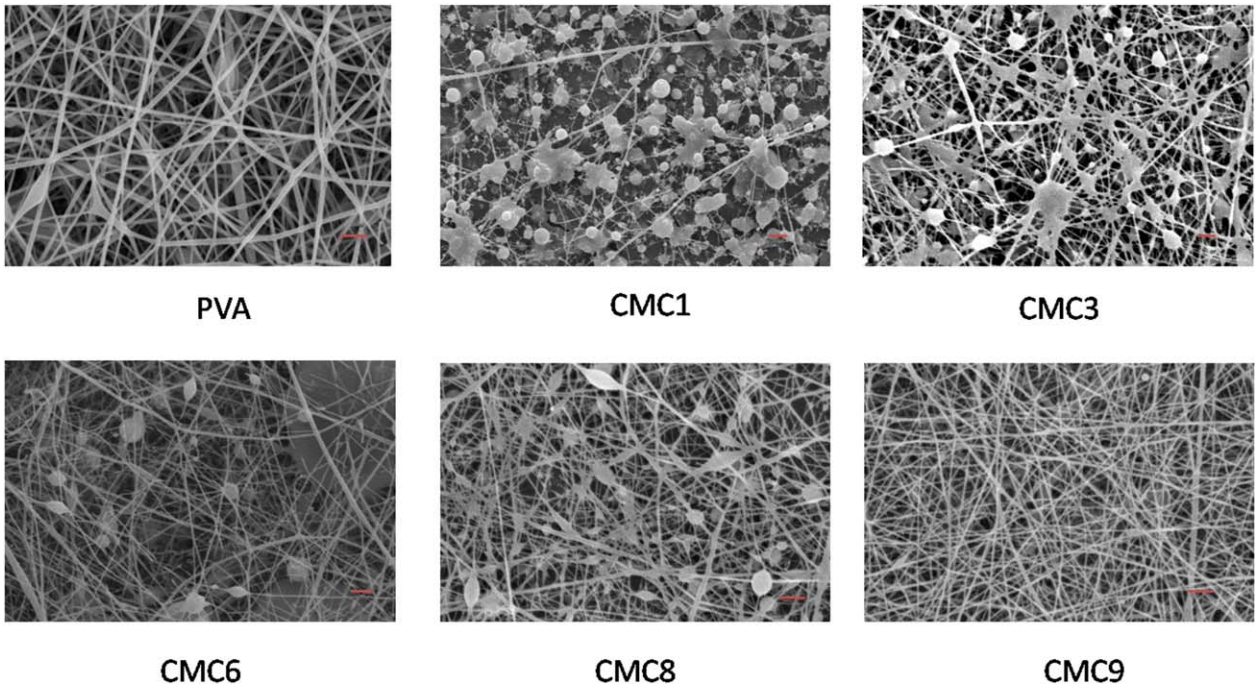

Figure 6. SEM images of crosslinked PVA, CMC1, CMC3, CMC6, CMC8 and CMC9 (CMCthe length of the scale bar is 1 μm). [Color figure can be viewed in the online issue, which is available at wileyonlinelibrary.com.]

membrane of CMC/PVA had characteristic absorbances of both PVA and CMC. The peak ~3400 cm^{-1} was due to the unbonded and hydrogen bonded —OH stretching band. The absorbance around 2900 cm^{-1} can be ascribed to the C—H stretching band. C═O of PVA located ~1720 cm^{-1}. The overlapped peak from the asymmetric stretching of —C═O (—COONa) and the bending vibration band of —NH_2 are located ~1560–1650 cm^{-1}.[37] Adsorption of C—O—C stretching was at 1060 cm^{-1}. After crosslinking, the peak of —NH_2 decreased somewhat owing to the Schiff reaction between —NH_2 and C═O. The other peaks had no obvious change. The peaks of newly formed C═N from the Schiff base and C═C of the polymerized glutaraldehyde overlapped with those of the original C═O from PVA and CMC.[18,38]

The SEM images of the crosslinked mats are shown in Figure 6. There were no obvious changes to the morphology of the membranes. This was more apparent for CMC9 which still had only fibers after crosslinking. The surface wettability(hydrophobicity/hydrophilicity)plays an important role on hemocompatibility of biomaterials owing to its effects on protein adsorption, platelet adhesion/activation, and blood coagulation.[39] The wettability of CMC/PVA was measured through water contact angles. As shown in Table II, before crosslinking, all the samples were highly hydrophilic showing a water contact angle of 28.1–56.5°. With the increase of CMC amount, the water contact angle decreased owing to the good hydrophilicity of —COOH, NH_2, and OH. After crosslinking, the water contact angle of all the samples increased. The wettability change was due to the heterogeneity of the reaction between the membrane and glutaraldehyde. The reaction happened on the surface of membrane; therefore, the amino group on the surface was blocked by the hydrophobic aliphatic group in which the long aliphatic chain prevented contact between water and the polymer chain, resulting in less interaction between the membrane and water, therefore inducing more hydrophobicity.[40] It is worthy to mention that CMC9 had the highest water contact angles 93.5° after crosslinking, while it had the lowest one (28.1°) before crosslinking. Water contact angle images of CMC9 and crosslinked CMC9 were shown in Figure 7. This confirmed that a dominant fraction of NH_2 group took part in the crosslinking, resulted in the higher degree of crosslinking, higher content of aliphatic groups, and higher hydrophobicity.[37]

Platelet adhesion experiment was carried out on CMC/PVA mats to measure the hemocompatibility of the electrospun mats. The SEM images of the mats after contacting with PRP for 2 h are shown in Figure 8. It was shown that there were platelet adhesion and aggregation on the mats of CMC1, CMC3, and CMC 6. For CMC9, there was much less platelet adhered

Table II. Water Contact Angle of the CMC/PVA Mats (°)

	PVA	CMC1	CMC3	CMC5	CMC6	CMC9
Before crosslinking	47.7 ± 1.2	56.5 ± 2.2	51.3 ± 2.0	48.8 ± 1.4	33.4 ± 1.5	28.1 ± 0.9
After crosslinking		71.8 ± 2.2	75.9 ± 2.3	75.6 ± 2.6	82.5 ± 1.9	93.5 ± 0.2

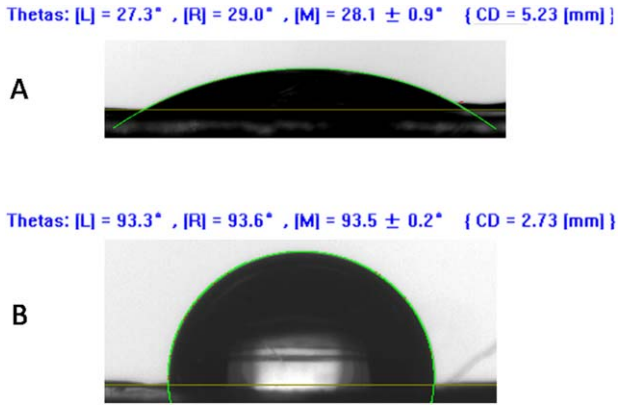

Figure 7. Water contact angle images of CMC9 (A) and crosslinked CMC9 (B). [Color figure can be viewed in the online issue, which is available at wileyonlinelibrary.com.]

and no platelet aggregation occurred. The results indicated that CMC9 had best hemocompatibility.

When platelets contact a foreign artificial surface, they are activated by the foreign material. Platelet activation induces a series of complex reactions that result in platelet adhesion and aggregation, leading to thrombus. Therefore, lower platelet adhesion on the material surface is a measure of better hemocompatibility. Physical and chemical characteristics of the foreign surface, such as chemical functionalities, surface charge, morphology, surface wettability, etc., can be correlated with platelet attachment and adhesion. Negatively charged surface are considered better, owing to the electrostatic repulsion between the surface and platelets that decreases platelet adhesion.[41] It is also accepted that materials with hydrophilic and hydrophobic microdomains, or graft compolymers having hydrophilic-hydrophobic chains with a degree of surface mobility, have good hemocompatibility.[42] The hydrophilic —OH, —COOH, —NH give rise to hydrophilic microdomain, while aliphatic —C═C—, —C═N, —$CH_2CH_2CH_2$— form hydrophobic domains and chains to block the contact of proteins and platelets with the material surface. Moreover, the morphology, especially on the micron and nanometer scale, influences protein adsorption, platelet adhesion, and blood coagulation.[43] The surfaces thus mimic the natural vessel inner surface and native extracellular matrix and possess good biocompatibility.[44] The highest negative charge of CMC9 would result in the highest repulsion between the mats and platelets. There are no beads on CMC9 in which nanofibers diameter of CMC9 of 100–200 nm are found, similar with that of extracellular matrix (50–500 nm). The negative charged surface and morphology similarity to the extracellular matrix might be the basis for the optimized hemocompatibility for CMC9.

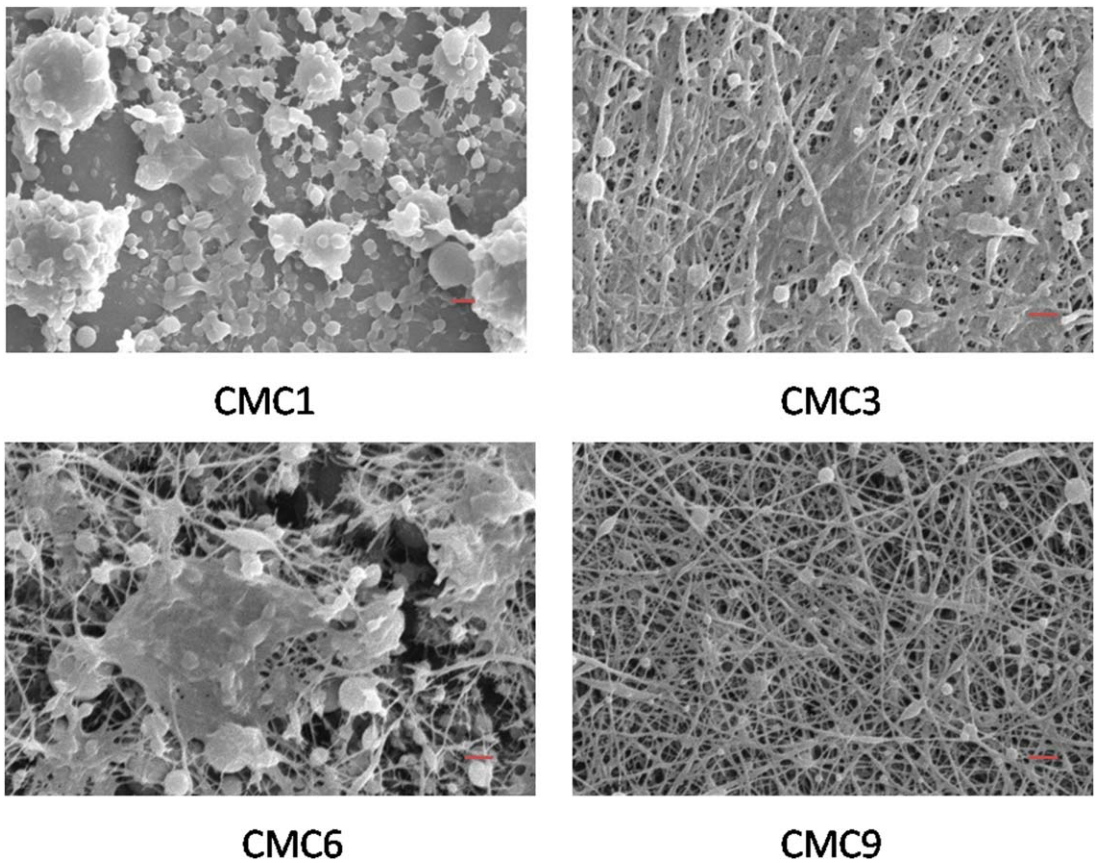

Figure 8. SEM images of the CMC/PVA electrospun mats (CMC1, CMC3, CMC6, and CMC9) after platelet adhesion (the length of the scale bar is 1 μm). [Color figure can be viewed in the online issue, which is available at wileyonlinelibrary.com.]

CONCLUSIONS

Chitosan was completely deacetylated and carboxymethylated to prepare O-carboxymethylchitosan. CMC/PVA mats with nanofibers were then successfully prepared through electrospinning blend solutions of CMC and PVA. The diameters of the fibers were in the range of 70–200 nm which after crosslinking with gluturaldehyde, provided a fibrous mat structure that remained although several samples expressed beading. Crosslinked CMC/PVA mats expressed good hemocompatibility according to the platelet adhesion results. The negatively charged chemical surface and the morphology similarity to the extracellular matrix are the main factors promoting the good hemocompatibility witnessed in this study. To fully assess the blood compatibility of CMC/PVA nanofibers and the corresponding mechanism, other tests, such as blood coagulation, protein adsorption, will be the subject of future studies.

ACKNOWLEDGMENTS

The authors acknowledge the National Science Foundation of China (Project No. 21264007, 21466011), and the Young Researcher Project of Hainan University (qnjj1221) for their financial support. We also thank Prof L.A. Lucia for helpful discussions regarding the preparation of the manuscript.

REFERENCES

1. Flemming, R.; Murphy, C.; Abrams, G.; Goodman, S.; Nealey, P. *Biomaterials* **1999**, *20*, 573.
2. Ma, Z.; Kotaki, M.; Inai, R.; Ramakrishna, S. *Tissue Eng.* **2005**, *11*, 101.
3. Park, K. E.; Jung, S. Y.; Lee, S. J.; Min, B. M.; Park, W. H. *Int. J. Biol. Macromol.* **2006**, *38*, 165.
4. Sill, T. J.; von Recum, H. A. *Biomaterials* **2008**, *29*, 1989.
5. Pham, Q. P.; Sharma, U.; Mikos, A. G. *Tissue Eng.* **2006**, *12*, 1197.
6. Salihu, G.; Goswami, P.; Russell, S. *Cellulose* **2012**, *19*, 739.
7. Branciforti, M. C.; Custodio, T. A.; Guerrini, L. M.; Averous, L.; Bretas, R. E. S. *J. Macromol. Sci. Part B* **2009**, *48*, 1222.
8. Thavasi, V.; Singh, G.; Ramakrishna, S. *Energy & Environ. Sci.* **2008**, *1*, 205.
9. Qin, X. H.; Wang, S. Y. *J. Appl. Polym. Sci.* **2006**, *102*, 1285.
10. Zheng, B.; Liu, G.; Yao, A.; Xiao, Y.; Du, J.; Guo, Y.; Xiao, D.; Hu, Q.; Choi, M. M. *Sensors Actuators B: Chem.* **2014**, *195*, 431.
11. Beachley, V.; Wen, X. *Mater. Sci. Eng. C* **2009**, *29*, 663.
12. Li, Q.; Dunn, E.; Grandmaison, E.; Goosen, M. *J. Bioact. Compat. Polym.* **1992**, *7*, 370.
13. Shukla, S. K.; Mishra, A. K.; Arotiba, O. A.; Mamba, B. B. *Int. J. Biol. Macromol.* **2013**, *59*, 46.
14. Jayakumar, R.; Prabaharan, M.; Nair, S.; Tamura, H. *Biotechnol. Adv.* **2010**, *28*, 142.
15. Zhao, Y.; Zhou, Y.; Wu, X.; Wang, L.; Xu, L.; Wei, S. *Appl. Surf. Sci.* **2012**, *258*, 8867.
16. Ding, F.; Deng, H.; Du, Y.; Shi, X.; Wang, Q. *Nanoscale* **2014**, *6*, 9477.
17. Shalumon, K.; Binulal, N.; Selvamurugan, N.; Nair, S.; Menon, D.; Furuike, T.; Tamura, H.; Jayakumar, R. *Carbohydr. Polym.* **2009**, *77*, 863.
18. Du, F.; Wang, H.; Zhao, W.; Li, D.; Kong, D.; Yang, J.; Zhang, Y. *Biomaterials* **2012**, *33*, 762.
19. Zhang, Y.; Huang, X.; Duan, B.; Wu, L.; Li, S.; Yuan, X. *Colloid. Polym. Sci.* **2007**, *285*, 855.
20. Ohkawa, K.; Cha, D.; Kim, H.; Nishida, A.; Yamamoto, H. *Macromol. Rapid Commun.* **2004**, *25*, 1600.
21. Kriegel, C.; Kit, K.; McClements, D. J.; Weiss, J. *Polymer* **2009**, *50*, 189.
22. Weber, N.; Wendel, H. P.; Ziemer, G. *Biomaterials* **2002**, *23*, 429.
23. Lin, W. C.; Yu, D. G.; Yang, M. C. *Colloids Surf. B: Biointerfaces* **2005**, *44*, 82.
24. Koh, L. B.; Rodriguez, I.; Venkatraman, S. S. *Biomaterials* **2010**, *31*, 1533.
25. Fedel, M.; Endogan, T.; Hasirci, N.; Maniglio, D.; Morelli, A.; Chiellini, F.; Motta, A. *J. Bioact. Compat. Polym.* **2012**, 0883911512446060.
26. Balan, V.; Verestiuc, L. *Eur. Polym. J.* **2014**, *53*, 171.
27. Lin, C. W.; Lin, J. C. *J. Biomater. Sci. Polym. Ed.* **2001**, *12*, 543.
28. Muzzarelli, R. A.; Giacomelli, G. *Carbohydr. Polym.* **1987**, *7*, 87.
29. Yin, X.; Chen, J.; Yuan, W.; Lin, Q.; Ji, L.; Liu, F. *Polym. Bull.* **2012**, *68*, 1215.
30. Chen, L.; Du, Y.; Zeng, X. *Carbohydr. Polym.* **2003**, *338*, 333.
31. Ge, H.; Luo, D. *Carbohydr. Polym.* **2005**, *340*, 1351.
32. Hou, X.; Wang, X.; Zhu, Q.; Bao, J.; Mao, C.; Jiang, L.; Shen, J. *Colloids Surf. B: Biointerfaces* **2010**, *80*, 247.
33. Chen, L.; Du, Y.; Wu, H.; Xiao, L. *J. Appl. Polym. Sci.* **2002**, *83*, 1233.
34. Zheng, M.; Han, B.; Yang, Y.; Liu, W. *Carbohydr. Polym.* **2011**, *86*, 231.
35. Du, J.; Hsieh, Y. L. *Nanotechnology* **2008**, *19*, 125707.
36. Lin, T.; Fang, J.; Wang, H.; Cheng, T.; Wang, X. *Nanotechnology* **2006**, *17*, 3718.
37. Monteiro, O. A.; Airoldi, C. *Int. J. Biol. Macromol.* **1999**, *26*, 119.
38. Reis, E. F.; Campos, F. S.; Lage, A. P.; Leite, R. C.; Heneine, L. G.; Vasconcelos, W. L.; Lobato, Z. I. P.; Mansur, H. S. *Mater. Res.* **2006**, *9*, 185.
39. Menzies, K. L.; Jones, L. *Optom. Vis. Sci.* **2010**, *87*, 387.
40. Beppu, M.; Vieira, R.; Aimoli, C.; Santana, C. *J. Membr. Sci.* **2007**, *301*, 126.
41. Hao, N.; Wang, Y. B.; Zhang, S. P.; Shi, S. Q.; Nakashima, K.; Gong, Y. K. *J. Biomed. Mater. Res. A* **2014**, *102*, 2972.
42. Xua, L.; Siedlecki, C. A. *Biomaterials* **2007**, *28*, 3273.
43. Lord, M. S.; Cheng, B.; McCarthy, S. J.; Jung, M.; Whitelock, J. M. *Biomaterials* **2011**, *32*, 6655.
44. Yaseen, M.; Zhao, X.; Freund, A.; Seifalian, A. M.; Lu, J. R. *Biomaterials* **2010**, *31*, 3781.